Structure and dielectric properties of the $(1-x)La(Mg_{1/2}Ti_{1/2})O_3-x(Na_{1/2}Bi_{1/2})TiO_3$ microwave ceramics

2006 J. Phys.: Condens. Matter 18 5703

(http://iopscience.iop.org/0953-8984/18/24/011)

INSTITUTE OF PHYSICS PUBLISHING JOURNAL OF PHYSICS: CONDENSED MATTER

J. Phys.: Condens. Matter **18** (2006) 5703–5713 doi:10.1088/0953-8984/18/24/011

Structure and dielectric properties of the $(1-x)La(Mg_{1/2}Ti_{1/2})O_3$–$x(Na_{1/2}Bi_{1/2})TiO_3$ microwave ceramics

Andrei N Salak[1] **and Victor M Ferreira**[2]

[1] Department of Ceramics and Glass Engineering/CICECO, University of Aveiro, 3810-193 Aveiro, Portugal
[2] Department of Civil Engineering/CICECO, University of Aveiro, 3810-193 Aveiro, Portugal

E-mail: salak@cv.ua.pt and victorf@civil.ua.pt

Received 16 February 2006, in final form 17 April 2006
Published 2 June 2006
Online at stacks.iop.org/JPhysCM/18/5703

Abstract

The $(1-x)La(Mg_{1/2}Ti_{1/2})O_3$–$x(Na_{1/2}Bi_{1/2})TiO_3$ perovskite ceramics ($0 \leqslant x \leqslant 0.6$) were characterized with respect to both crystal structure and dielectric properties. The crystal structure of the solid solutions was investigated by x-ray diffraction (XRD) and the sequence of composition-driven structure transformations was revealed: $P2_1/n$ ($0 \leqslant x \leqslant 0.2$), a coexistence of $Pnma$ and $R\bar{3}c$ (at the vicinity of $x = 0.3$), and $R\bar{3}c$ ($0.4 \leqslant x \leqslant 0.6$). The dielectric response of the ceramics was measured as a function of temperature and composition. The range between $x = 0.3$ and 0.4, where the temperature coefficient of the resonant frequency passes the zero value, is associated with a discontinuous phase transition between orthorhombic and rhombohedral structure modifications. The compositional variation of the fundamental dielectric parameters, estimated at different frequency ranges, is discussed in relation to the crystal chemistry of the system.

1. Introduction

Non-cubic complex perovskites $A(B'_mB''_{1-m})O_3$ (A = La, Sr, Ca), particularly those that are B-site ordered, could be promising for microwave applications owing to their very high values of quality factor (Q) at resonant frequency (f_0) in the gigahertz range [1]. However, as a result of their distorted crystal structure due to tilted oxygen octahedra, these compounds are characterized by a negative temperature coefficient of the resonant frequency (τ_f) [2, 3]. Both their relative permittivity (ε'_r, mostly within 20–30) and τ_f have been shown to be improved by forming solid solutions with dipole-ordered perovskites like ferroelectrics or incipient ferroelectrics [4–6].

Nowadays, $(Na_{1/2}Bi_{1/2})TiO_3$ (NBT) is considered to be a parent component for lead-free ferroelectric and piezoelectric materials [7, 8]. At the same time, undoped NBT demonstrates

too high a loss and a large coercive field, which produce difficulties for poling [8, 9]. In solid solutions with high-Q microwave perovskite $La(Mg_{1/2}Ti_{1/2})O_3$ (LMT), promising dielectric properties were recently revealed for NBT-rich compositions [10]. Doping with as low as 5 mol% LMT was found to decrease radio-frequency dielectric loss by a factor of 20. Increasing the amount of LMT in NBT (up to 25 mol%) results in a minor change in its crystal structure: from $R3c$ to higher-symmetry $R\bar{3}c$ [10]. Both space groups allow antiphase octahedral tilting ($a^-a^-a^-$ in Glazer's notation [11]) only. Since the crystal structure of LMT is monoclinic $P2_1/n$ ($a^-b^+a^-$) [12], one can expect a sequence of structure transformations involving oxygen octahedral tilting in the LMT-rich side of the $(1-x)$LMT–xNBT system. Such transformations in complex perovskites and their solid solutions are known to alter the slope of the temperature dependence of relative permittivity and hence change the sign of τ_f [2, 3]. Thus, the addition of sodium bismuth titanate can compensate the negative value of τ_f for lanthanum magnesium titanate. Moreover, due to the high polarizability of Bi^{3+}, the relative permittivity of the $(1-x)$LMT–xNBT ceramics is supposed to increase with x. It is also expected that NBT-containing compositions have lower sintering temperature in comparison with that of pure LMT ceramics (as high as 1870 K) [13].

In addition to the evident applied aspect of this work, there is interest in the $(1-x)$LMT–xNBT system as a model object. The investigations performed on these ceramics continue our systematic studies of LMT-based perovskite solid solutions LMT-$ATiO_3$ (where A = Ba, Sr, and La) [5, 6, 12]. These studies are aimed at clarifying the contributions to the fundamental microwave parameters (ε_r', τ_f and Qf_0) resulting from dilution of the average atomic polarizability and crystal structure transformations in the compositions derived from low-loss complex perovskite dielectrics.

The present work reports on the structure and dielectric characterization of the $(1-x)$LMT–xNBT ceramics ($0 \leqslant x \leqslant 0.6$). The compositional variation of the microwave dielectric properties is discussed with respect to the crystal chemistry of the LMT–NBT perovskite system.

2. Experimental details

The conventional mixed oxide method was used to process powders of $(1-x)$LMT–xNBT. A stoichiometric mixture of the respective reagent-grade oxides and carbonates was ball-milled in ethanol and calcined at 1020 K (for 4 h) and then at 1220 K (4 h) with intermediate regrindings. The powders were then isostatically pressed into disks of 10 mm in diameter and about 1 mm in thickness and sintered in air at the temperatures at which the highest density is achieved. The sintering temperatures ranged from 1470 K for $0.4 \leqslant x \leqslant 0.6$ to 1820 K for $x = 0.1$. The dwell time was 4 h; heating and cooling rates were 5 K min^{-1} in every case. For microwave dielectric measurements, cylindrical samples of 10 mm in diameter and 8–12 mm length were pressed and sintered under the same conditions. The relative density of the sintered samples was determined by the Archimedes method.

Phase analysis of the ceramics and crystal structure determination were performed by x-ray diffraction (XRD) from powders ground from the samples. XRD data were collected at room temperature using a Rigaku D/MAX-B diffractometer (with Cu Kα radiation; a tube power of 40 kV, 30 mA; and a graphite monochromator). Rietveld refinement of the data that was obtained was performed using the FULLPROF suite [14].

The samples for dielectric investigation were polished to form disks with a thickness of 0.4–0.5 mm, electroded with platinum paste, and annealed at 1270 K. The dielectric permittivity and loss tangent were measured as a function of temperature within a frequency range of 10^2–10^6 Hz using a Precision LCR meter (HP 4284A) and an Impedance/Gain-

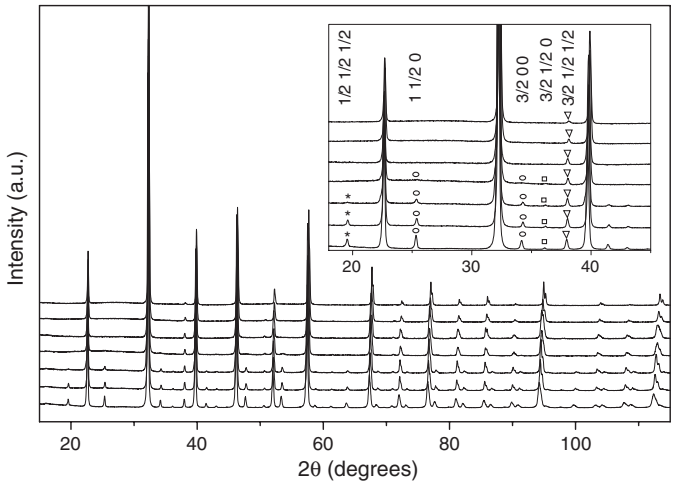

Figure 1. XRD patterns of $(1-x)$LMT–xNBT ($x = 0$, 0.1, 0.2, 0.3, 0.4, 0.5, and 0.6, from bottom to top). The inset shows the superstructure reflections, indicating Mg/Ti ordering ($*$), antiparallel A-cation displacements (○), in-phase octahedral tilting (□), and antiphase octahedral tilting (∇).

Phase Analyzer (Solartron 1260). The measurements were performed over the interval 10–820 K on both heating and cooling, with a rate of 1.5 K min^{-1}, using a cryostat (Displex APD Cryogenics, 10–300 K), an environment chamber (Delta Design 9023, 95–480 K) and a furnace (300–820 K). The room-temperature permittivity, Q factor and resonant frequency of the samples in the microwave frequency range were estimated by an adaptation of the Hakki–Coleman method [15, 16] using a 10 MHz–20 GHz Scalar Analyzer (IFR 6823).

3. Results and discussion

Analysis of XRD data of the sintered ceramics revealed that single-phase perovskite solid solutions are obtained under the above-mentioned sintering conditions. Taking into account the previous study performed on the NBT-rich side of the system [10], one may conclude that the perovskite phase is formed over the whole compositional range of $(1-x)$LMT–xNBT.

The crystal structure of the LMT perovskite has been refined to have monoclinic symmetry with $P2_1/n$ space group [17]. Based on this space group, both rocksalt-type Mg/Ti cation ordering and $a^-b^+a^-$ octahedral tilting can be described. In the XRD patterns of the $(1-x)$LMT–xNBT ceramics, the respective superstructure reflections associated with B-site ordering, A-cation antiparallel displacement, and both in-phase and antiphase octahedral tilting were observed for the compositions with $x \leqslant 0.2$ (figure 1). Therefore, the $P2_1/n$ space group was used for the crystal structure refinement of the LMT-rich compositions ($x = 0.1$ and 0.2).

Further dilution of LMT with NBT ($0.2 < x < 0.3$) results in the vanishing of the (1/2 1/2 1/2) superstructure reflection[3] (figure 1). This is apparently related to the disappearance of long-range B-cation ordering. At this compositional range, the Mg/Ti ratio becomes far enough from 1 and perfect alternation of these atoms is no longer provided, hence there could be a short-range ordering only. At the same time, the other superstructure reflections, namely those originating from antiparallel displacements of A-site cations $-1/2$ (eeo, eoe, oee; where o—odd, e—even), in-phase octahedral tilting $-1/2$ (ooe, oeo, eoo) and antiphase

[3] Hereafter, the indexing is presented in the primitive perovskite unit cell.

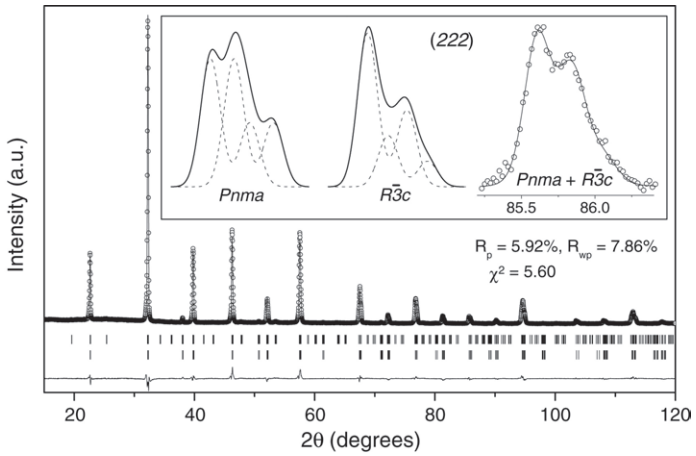

Figure 2. Observed (○), calculated (solid line), and difference (below) patterns of the room-temperature XRD data, along with the calculated peak positions (vertical bars) for the composition $x = 0.3$. The inset compares profiles of the (222) fundamental reflection generated for the $Pnma$, $R\bar{3}c$ space group and calculated using the two-phase model ($Pnma + R\bar{3}c$).

tilting $-1/2$ (ooo, $h + k + l > 3$) are still present in the XRD pattern (the inset in figure 1). One may suppose that the solid solution with $x = 0.3$ is characterized by the same tilt configuration ($a^-b^+a^-$) as the above-considered compositions, with smaller NBT content. Thus, in order to solve the crystal structure of the composition $x = 0.3$, the $Pnma$ space group was chosen preliminarily. The refined pattern looked satisfactory; quite good values of the refinement quality factors were obtained. However, detailed analysis of the calculated XRD intensities revealed some inaccuracies in the description of the high-angle fundamental reflections. In particular, the observed profiles of the (222) and (400) reflections failed to be described adequately. Another probable space group which allows both in-phase and antiphase tilt configuration in the absence of B-site cation ordering, $Cmcm$ [18], was tried; however, the refinement did not yield acceptable results.

When considering XRD patterns of the ceramics with NBT content higher than 30 mol%, one can notice a disappearance of the superstructure reflections associated with both A-site cation displacements and in-phase octahedral tilting (the inset in figure 1). At the same time, those reflections related to antiphase octahedral tilting are present. On the basis of the observed tilt configuration as well as the shape (splitting type) of the fundamental reflections, the crystal structure of the $(1-x)$LMT–xNBT ceramics with $x = 0.4$, 0.5 and 0.6 was successively solved using the $R\bar{3}c$ space group (tilt system $a^-a^-a^-$). The $Imma$ space group ($a^-b^0a^-$) was also tested, but the refinement using the former model gave significantly a better fit with respect to both the description of the XRD profiles and the values of the refinement quality factors.

Turning back to the crystal structure of the composition $x = 0.3$, one may suppose that this solid solution actually consists of two perovskite phases of similar chemical composition. Indeed, the profiles of the most indicative fundamental reflections, such as (hhh) and (h00), could not be described adequately using a particular possible space group. For instance, a multiplicity of (222) reflections when using $Pnma$ (a doublet with the intensity ratio 1:1) results in the certain profile shown in the inset in figure 2. In the case of the $R\bar{3}c$ space group, this reflection is a doublet, with the intensity ratio 2:1 (ibidem). Superposition of these reflections could provide the resulting reflection shape. Indeed, crystal structure refinement using the two-phase model ($Pnma + R\bar{3}c$) was successful, with correct descriptions of all

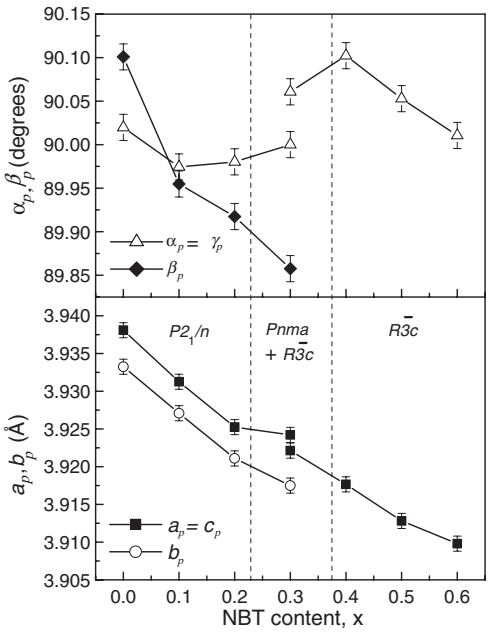

Figure 3. Primitive perovskite unit-cell parameters (a_p, b_p, c_p and α_p, β_p, γ_p) as a function of NBT content in the $(1-x)$LMT–xNBT system.

Table 1. Crystal structure parameters of the $(1-x)$LMT–xNBT system obtained from refinement of the room-temperature XRD data. (The data for LMT ($x = 0$) were taken from [17].)

x	Space group	a (Å)	b (Å)	c (Å)	β (deg)	V (Å^3)	Z
0	$P2_1/n$	5.5644(10)	5.5742(10)	7.8665(20)	90.03(1)	243.998(10)	2
0.1	$P2_1/n$	5.5618(10)	5.5574(10)	7.8542(10)	89.96(2)	242.769(10)	2
0.2	$P2_1/n$	5.5551(10)	5.5471(10)	7.8422(10)	89.97(2)	241.658(10)	2
0.3	$Pnma$	5.5428(10)	7.835(1)	5.5566(10)		241.307(9)	4
0.3	$R\bar{3}c$	5.5496(12)		13.5723(10)		362.006(8)	6
0.4	$R\bar{3}c$	5.546(13)		13.5455(10)		360.769(9)	6
0.5	$R\bar{3}c$	5.5361(10)		13.5419(12)		359.432(10)	6
0.6	$R\bar{3}c$	5.5298(10)		13.5415(10)		358.604(12)	6

the observed intensities (figure 2). The relative amounts of the $Pnma$ and $R\bar{3}c$ phases in ceramics with $x = 0.3$ were estimated to be 59% and 41%, respectively. The phenomenon is rather unusual but not unique: the coexistence of orthorhombic and rhombohedral phases was observed in La-based compounds in both compositional [19] and temperature ranges [20].

Based on the refined structure data (table 1) and the unit cell relations reported in [12], the parameters of the primitive perovskite unit cell were calculated. These are presented in figure 3 as a function of NBT content. Figure 4 shows the compositional variation of the primitive perovskite unit cell volume. As is seen, there is a discontinuity in the dependence of the parameters on NBT content in the vicinity of $x = 0.3$, whereas both before and after this composition these parameters vary gradually. The observed behaviour is consistent with the results of group-theoretical analysis [21]. Indeed, the $P2_1/n \rightarrow Pnma$ phase transition is

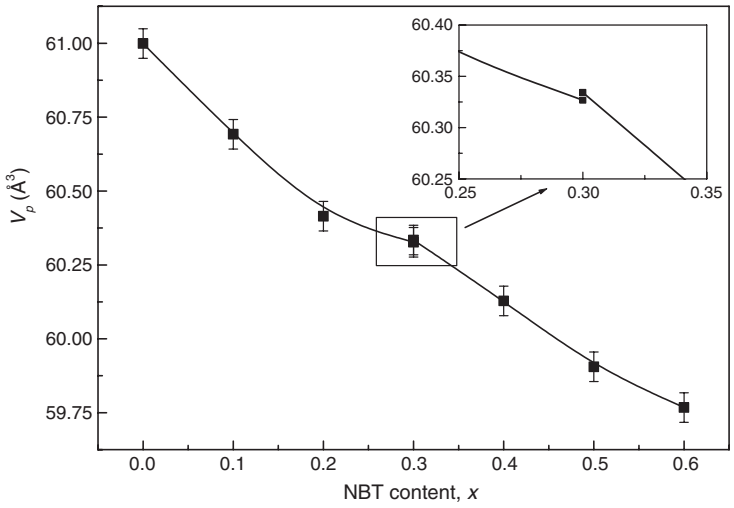

Figure 4. Variation of primitive perovskite unit cell volume with composition for the $(1-x)$LMT–xNBT ceramics.

allowed by Landau theory to be continuous [12] and the $Pnma \rightarrow R\bar{3}c$ crossover is required to be discontinuous. It should be noted that the intermediate phase with the symmetry $Imma$ ($a^-b^0a^-$) was not revealed in the system studied. The phase of this symmetry was found in the solid solutions based on LMT [6, 12]. The intermediate tile configuration $a^-b^0a^-$ between orthorhombic $a^-b^+a^-$ and rhombohedral $a^-a^-a^-$ seems to be natural. Nevertheless, the $Imma$ phase either does not exist in the $(1-x)$LMT–xNBT system or its composition range is too narrow to be detected. At the same time, the direct compositional phase transition $Pnma \rightarrow R\bar{3}c$ in complex perovskites has also been reported by Kennedy *et al* [22].

A possible reason for the discontinuity can be an increasing role of Bi^{3+} in the chemical bond of $(1-x)$LMT–xNBT. At $x = 0.3$, the relative amount of Bi is close to one per six primitive perovskite unit cells. As the B-cation coordination number is six, this means that Bi–O–Bi chains may appear in this composition range. It is known that Bi^{3+} (as well as Pb^{2+}), owing to their $6s^2$ electronic configuration, are inclined to form a covalent chemical bond in oxide solids [23]. That is why a number of complex oxides with bismuth or lead as an A-site cation crystallize to a pyrochlore-type structure rather than a perovskite structure. Besides, the 'covalence-inducing' feature of these cations is associated with ferroelectricity in Pb- and Bi-containing compositions. In the case of the $(1-x)$LMT–xNBT perovskite system, an asymmetric coordination of Bi^{3+} can result in a non-monotonic variation in the unit cell dimensions.

The phase transition between the $Pnma$ and $R\bar{3}c$ modifications was also revealed by measurements of the radio-frequency dielectric response as a function of temperature. The temperature variation of the relative permittivity for the ceramics measured at 1 MHz is shown in figure 5. No substantial anomalies are observed within the presented temperature interval for all the compositions that were studied, except for that with $x = 0.3$. The curve for ceramics with $x = 0.3$ alters slope at about 500 K, suggesting a first-order phase transition. In the ranges where $\varepsilon'_r(T)$ for all the compositions varies almost linearly, the thermal coefficient of capacitance (τ_C) was evaluated. The values of τ_f were then determined by using the relation $\tau_f = -1/2[\tau_C + \alpha_L]$ [24]. The linear thermal-expansion coefficient (α_L) was assumed to be 10 ppm K^{-1}, as its value is ordinarily in the range 9–12 ppm K^{-1} for most perovskites [2].

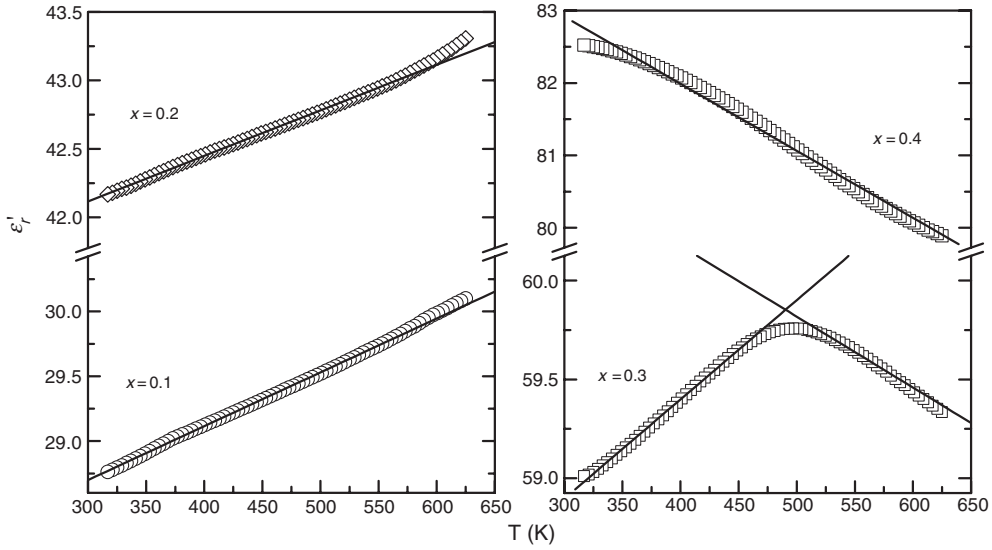

Figure 5. Temperature dependences of relative permittivity (ε'_r) for the $(1-x)$LMT–xNBT ceramics measured on cooling at 1 MHz. (Open symbols and solid lines represent experimental data and the linear fit, respectively.)

Table 2. Microwave dielectric properties in the $(1-x)$LMT–xNBT system measured at room temperature. (The data for LMT ($x = 0$) were taken from [6]. The microwave measurements for the composition $x = 0.6$ could not be performed, because the dielectric loss in the gigahertz range was higher than the limit allowed by the resonance method used.)

x	Relative density (%)	ε'_r	f_0 (GHz)	Q (GHz)
0	97	27.6	7.10	114 312
0.1	89	27.9	8.27	5 259
0.2	92	39.5	7.29	1 812
0.3	91	56.9	5.95	906
0.4	94	75.4	4.90	570
0.5	93	102.9	4.12	390

The relative permittivity as well as the quality factor of the $(1-x)$LMT–xNBT ceramics were also measured in the microwave frequency range (table 2). An unexpectedly huge reduction in the Qf_0 magnitude with increasing NBT content is observed. One of the reasons for the high dielectric loss may be vacancies appearing due to volatilization of Bi and/or Na from LMT–NBT when sintering at elevated temperatures. It is known that for the microwave dielectric characteristics, in particular, loss can be improved by appropriate doping and optimization of the processing conditions. The present work was not focused on this problem; no attempt was made to improve the Qf_0 value. In order to estimate the lattice (intrinsic) contribution to the observed permittivity and loss, far-infrared spectroscopy studies will be performed. These investigations are in progress and will be reported elsewhere.

The fundamental dielectric parameters estimated by different methods are presented in figure 6. The relative permittivity measured both in the gigahertz range and at 1 MHz is seen to follow the same hyperbolic-like dependence. It has recently been shown that such a hyperbolic-type dependence on composition, revealed in a number of dielectric binary solid

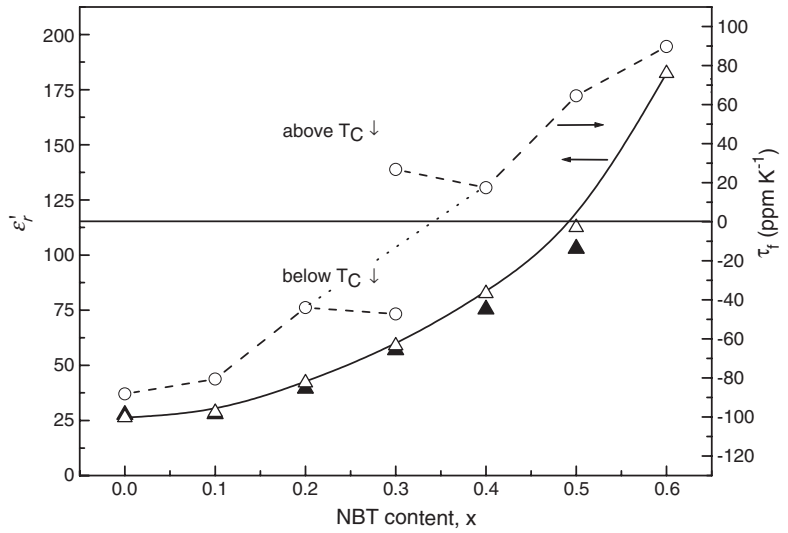

Figure 6. Room-temperature values of relative permittivity (ε'_r, triangles) and the temperature coefficient of the resonant frequency (τ_f, circles) for the $(1-x)$LMT–xNBT system measured in the gigahertz range (solid symbols) and the megahertz range (open symbols).

solutions, may be deduced from the Clausius–Mossotti equation, provided that the average unit cell polarizability is a linear function of the composition [5, 6]. As is seen from figure 6, the ε'_r values estimated in the radio-frequency range are regularly higher than those in the microwave range, and the difference between the values increases with x. This fact suggests that the increasing amount of sodium bismuth titanate (and thereby Bi^{3+}) causes the localized charge carriers in the $(1-x)$LMT–xNBT ceramics. The hopping conduction of these charges may contribute to the low-frequency dielectric response of the measured samples.

The τ_f values are also shown in figure 6 as a function of NBT content. Except for the composition $x = 0.3$, $\tau_f(x)$ varies in a monotonic way. As mentioned above, the τ_f values were estimated from the temperature variation of the relative permittivity. It should be taken into account that the curve's slope, $\Delta\varepsilon'_r/\Delta x$, increases when approaching the phase transition from both below and above. Therefore, the τ_f values calculated for the composition $x = 0.3$ (see figure 5) obviously fall outside the common trend.

Examination of $\varepsilon'_r(T)$ for the composition $x = 0.2$ (figure 5) revealed a deviation from the linear dependence in the high-temperature range ($T > 600$ K), which could testify to an approaching phase transition. So, dielectric measurements over an extended range were performed. Indeed, an anomaly in the temperature dependence of the relative permittivity with a temperature hysteresis typical of a first-order (discontinuous) crossover was observed (figure 7). The temperature (T_C) of the assumed phase transition from the $Pnma$ ($a^-b^+a^-$) to the $R\bar{3}c$ ($a^-a^-a^-$) modification was estimated to be about 730 and 490 K for the compositions with $x = 0.2$ and 0.3, respectively. Simple linear extrapolation to $x = 0$ gives a value of about 1210 K for pure LMT, which is in reasonable agreement with the value $T_C = 1170$ K reported by Levin *et al* [25]. Based on the extrapolation, one can expect a similar phase transition for the composition $x = 0.4$ at about 250 K. As seen from figure 5, a deviation of the respective $\varepsilon'_r(T)$ from the linear trend is in fact observed at $T < 350$ K. Supplementary dielectric measurements performed over a low-temperature range unexpectedly revealed a frequency-dependent behaviour of the dielectric response that is typical of relaxors (figure 8). The

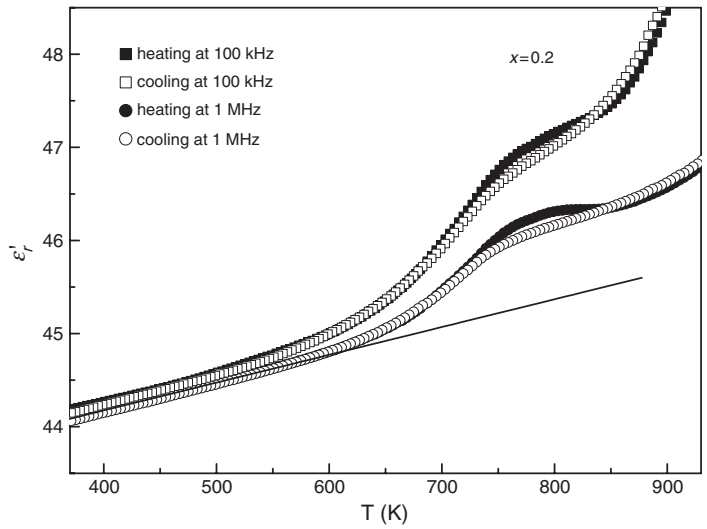

Figure 7. Relative permittivity of the composition $x = 0.2$ measured as a function of temperature in the radio-frequency range. (Solid line represents a linear fit.)

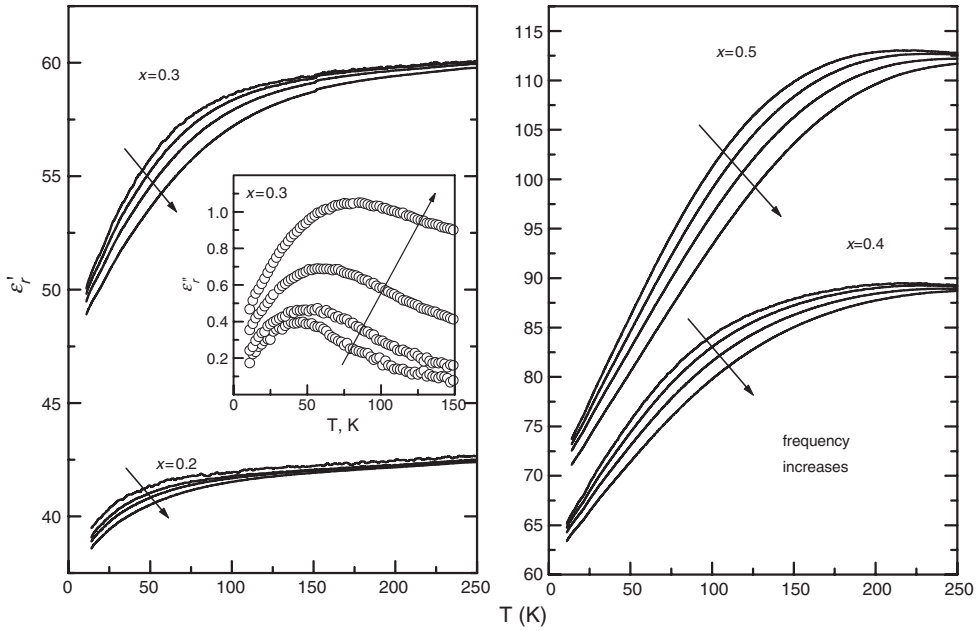

Figure 8. Low-temperature dielectric response of the $(1-x)$LMT–xNBT ceramics in the range 10^3–10^6 Hz. Inset: imaginary part of the dielectric response (ε_r'') of the composition $x = 0.3$ as a function of temperature.

temperature range where the permittivity is pronouncedly frequency-dispersive shifts with x and becomes undetectable for the composition $x = 0.1$. The appearance and localization of the dispersive ranges are certainly associated with the amount of NBT in the system. The origin of

this phenomenon in LMT–NBT is worthy of detailed investigation. It is evident that the same mechanism can contribute to the microwave dielectric loss of the ceramics at room temperature.

At the same time, these regions of the frequency-dependent behaviour of ε'_r appear to be directly related to the dispersive shoulder on the $\varepsilon'_r(T)$ curve observed previously for NBT and NBT-rich compositions in the $(1-x)$LMT–xNBT system [10]. Therefore, the observed low-temperature relaxation should be considered particularly in the context of the dielectric properties of NBT-rich compositions of the system. This is a matter for a separate investigation in the future.

4. Conclusions

Perovskite solid solutions were obtained in the quasi-binary $(1-x)$LMT–xNBT system in the compositional range $0 \leqslant x \leqslant 0.6$. An increasing amount of NBT in the system results in the following phase transformations: monoclinic $P2_1/n$ ($0 \leqslant x \leqslant 0.2$)—orthorhombic $Pnma$ (at about $x = 0.3$)—rhombohedral $R\bar{3}c$ ($0.4 \leqslant x \leqslant 0.6$). These are related to the disappearance of B-site cation ordering (at $x > 0.2$) and the change of the oxygen octahedral tilt configuration from $a^-b^+a^-$ ($x < 0.3$) to $a^-a^-a^-$ ($x > 0.3$). In the vicinity of $x = 0.3$, orthorhombic $Pnma$ and rhombohedral $R\bar{3}c$ phases coexist.

The compositional variation of ε'_r for the $(1-x)$LMT–xNBT system obeys a hyperbolic-like dependence. The coefficient τ_f alters its sign at x between 0.3 and 0.4, where a discontinuous phase transition between orthorhombic and rhombohedral modifications occurs. High ε'_r and near-zero τ_f values are achieved in solid solutions close to this compositional range; however, their dielectric loss is too high at microwave frequencies.

The low-temperature dielectric response of the $(1-x)$LMT–xNBT ceramics ($0.2 \leqslant x \leqslant 0.6$) is frequency-dependent. The temperature range of dispersive dielectric permittivity regularly shifts to higher temperatures as the amount of NBT is increased. This dielectric relaxation process is believed to contribute to the microwave dielectric loss of the ceramics at room temperature.

Acknowledgments

The assistance of Dr D D Khalyavin with crystal structure refinement and Dr N P Vyshatko with dielectric measurements is greatly appreciated. The first author also acknowledges the Foundation for Science and Technology (FCT-Portugal, grant SFRH/BPD/14988/2004) for their financial support.

References

[1] Sebastian M T, Axelsson A-K and Alford N McN 2005 List of microwave dielectric resonator materials and their properties http://www.lsbu.ac.uk/dielectric-materials/ and references therein
[2] Colla E L, Reaney I M and Setter N 1993 *J. Appl. Phys.* **74** 3414
[3] Reaney I M, Colla E L and Setter N 1994 *Japan. J. Appl. Phys.* **33** 3984
[4] Levin I, Chan J Y, Maslar J E, Vanderah T A and Bell S M 2001 *J. Appl. Phys.* **90** 904
[5] Salak A N, Seabra M P, Ferreira V M, Ribeiro J L and Vieira L G 2004 *J. Phys. D: Appl. Phys.* **37** 914
[6] Seabra M P, Salak A N, Ferreira V M, Vieira L G and Ribeiro J L 2004 *J. Eur. Ceram. Soc.* **24** 2995
[7] Gomah-Pettry J R, Marchet P, Salak A, Ferreira V M and Mercurio J P 2004 *Integr. Ferroelectr.* **61** 159
[8] Nagata H, Yoshida M, Makiuchi Y and Takenaka T 2003 *Japan. J. Appl. Phys.* **42** 7401
[9] Herabut A and Safari A 1997 *J. Am. Ceram. Soc.* **80** 2954
[10] Salak A N, Vyshatko N P, Kholkin A L, Ferreira V M, Olekhnovich N M, Radyush Yu V and Pushkarev A V 2006 *Mater. Sci. Forum* **514** 250

[11] Glazer A M 1975 *Acta Crystallogr.* A **31** 756
[12] Salak A N, Khalyavin D D, Mantas P Q, Senos A M R and Ferreira V M 2005 *J. Appl. Phys.* **98** 034101
[13] Seabra M P and Ferreira V M 2002 *Mater. Res. Bull.* **37** 255
[14] Rodriguez-Carvajal J 1993 *Physica* B **192** 55
[15] Hakki B W and Coleman P D 1960 *IRE Trans. Microw. Theory Tech.* **8** 402
[16] Kobayashi Y and Katoh M 1985 *IEEE Trans. Microw. Theory Tech.* **33** 586
[17] Avdeev M, Seabra M P and Ferreira V M 2002 *J. Mater. Res.* **15** 1112
[18] Woodward P M 1997 *Acta Crystallogr.* B **53** 32
[19] Hrovat M, Bernik S, Holc J, Kuscer D and Kolar D 1997 *J. Mater. Sci. Lett.* **16** 143
[20] Beznosov A B, Desnenko V A, Fertman E L, Ritter C and Khalyavin D D 2003 *Phys. Rev.* B **68** 054109
[21] Howard C J and Stokes H T 1998 *Acta Crystallogr.* B **54** 782
[22] Kennedy B J, Howard C J, Thorogood G J, Mestre M A T and Hesler J R 2000 *J. Solid State Chem.* **155** 455
[23] Goodenough J B, Kafalas J A and Longo J M 1972 *Preparative Methods in Solid State Chemistry* ed P Hagenmuller (New York: Academic) chapter 1
[24] Harrop P J 1969 *J. Mater. Sci.* **4** 370
[25] Levin I, Vanderah T A, Amos T G and Maslar J E 2005 *Chem. Mater.* **17** 3273